Lossy Mode Resonance Based Fiber Optic Sensors

Nidhi Paliwal and Joseph John

Abstract In the past couple of years, lossy mode resonance (LMR) phenomena has attracted the attention of researchers with its promising benefits in the field of fiber optic sensing. LMR based sensors have become a useful tool in sensing applications ranging from physical sensing to biosensing in a short span of time. In addition to sensing, LMR phenomena can also be utilized as wavelength filters for communication purposes. LMR based sensors are able to work independently of the specific polarization of light for sensing operations. Also, unlike evanescent wave and surface plasmon resonance (SPR) based sensors, the sensitivity of these LMR sensors does not get affected by the geometrical parameters of fiber and primarily depends on the thickness of thin film material. Till date, various geometries of fiber probes such as straight, D-shaped, tapered etc., have been explored. Bending and tapering of multimode fiber based LMR sensors improve the detection accuracy without affecting their sensitivity. However, in single mode fiber based LMR sensors the side polishing and tapering of fibers improve both the detection accuracy and sensitivity. Another method to improve the sensitivity is by using two LMR supporting thin film layers of higher refractive index instead of one. This chapter describes the theory and developments made in the field of LMR based fiber optic sensors for various sensing applications. Finally, future scope of the LMR sensing technology and possible research in this emerging area are suggested.

1 Introduction

Fiber optic sensing technology has been very popular in the past few decades with its promising benefits. Use of low cost optical sources and detectors in place of conventional devices for measuring various physical, chemical, and biological parameters has resulted in great economical benifts. One of the important reasons for the

N. Paliwal (✉) · J. John
Department of Electrical Engineering, Indian Institute of Technology Bombay,
Mumbai 400076, India
e-mail: nidhi83paliwal@gmail.com

I.R. Matias et al. (eds.), *Fiber Optic Sensors*, Smart Sensors,
Measurement and Instrumentation 21, DOI 10.1007/978-3-319-42625-9_2

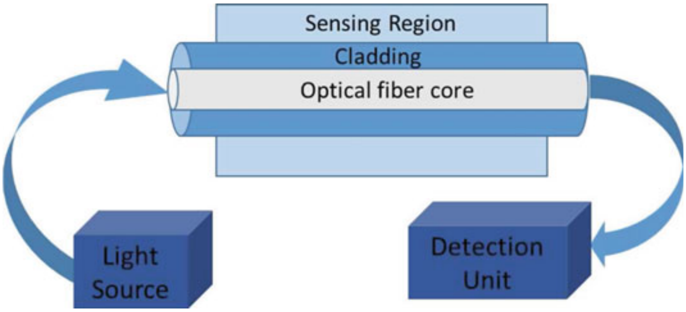

Fig. 1 Schematic representation of fiber optic sensor system

increased demand for fiber optic sensors is its pure dielectric nature due to which they can be effortlessly used in many perilous areas where conventional sensors may not work effectively. Another adavantage, especially for remote sensing and telemetry applications is the fast response of fiber optic sensors which makes it possible to send large amount of sensing information over long distances via optical fibers [1–4]. A typical fiber optic sensing system shown in Fig. 1 consists of a light source, fiber as a sensing element and a detector. Light is transmitted from a light source and passes through an optical fiber sensing probe, which senses change in the desired environmental parameter. The sensor modulates one or more characteristics of light viz, intensity, wavelength, amplitude or phase and then the modulated light is transmitted from the sensor to a signal processor, which in turn converts it into a signal for processing. In order to modulate the properties of light, optical waveguides coated with metal and semiconductors have been very popular [5–8]. It is known that the propagation of light in a medium depends on its properties. In optical fiber sensors, the medium for the propagation of light rays is an optical fiber. If fiber cladding is removed and some other thin film material is deposited over the unclad portion, it introduces losses in the light propagation and the extent of these losses depend upon the properties of thin film material.

2 Theory of LMR

2.1 Selection of Thin Film Material for Generation of LMR

Though LMR is similar to the other well established resonance phenomenon of SPR, there is a basic difference between these two resonance phenomena. Thin film material conditions for generating the surface plasmon modes and the lossy modes which eventually leads to the phenomenon of SPR and LMR respectively, are completely different. The permittivity of any thin film material is given by

$$\epsilon = \epsilon_r + i\epsilon_i \tag{1}$$

Table 1 LMR and SPR generating conditions

Phenomenon	Resonance condition	Suitable thin film materials
LMR	$\epsilon_r = +ive$ and $\lvert\epsilon_r\rvert > \epsilon_i, \epsilon_s$	Polymers, semiconductors, dielectrics, etc.
SPR	$\epsilon_r = -ive$ and $\lvert\epsilon_r\rvert > \epsilon_i, \epsilon_s$	Metals, semiconductors

where ϵ_r is the real part and ϵ_i is its imaginary part. For a given ϵ_s which is the permittivity of any surrounding medium, Table 1 defines the different conditions under which LMR and SPR can be generated. Thin film materials can be classified into two categories depending upon the resonance phenomena as shown in Table 1. LMR is generated when the real part of permittivity is positive and also higher in magnitude than both the permittivity of surrounding medium and its imaginary part. On the other hand, SPR is generated when the real part of thin film's permittivity is negative and also higher in magnitude than both the permittivity of surrounding medium and its imaginary part. There are also some materials whose real part is approximately zero and imaginary part of thin film permittivity is very large. These materials are suitable for generating long range surface exciton polariton. However, these are not in the scope of our studies because the choice of such materials is very limited.

2.2 Surface Plasmons and Surface Plasmon Resonance

Surface plasmons or surface plasma waves are electromagnetic modes associated with a metal-dielectric interface. Any metal thin film coated glass substrate in contact with a dielectric media supports charge density oscillations. These charge density oscillations along the metal-dielectric interface are known as surface plasma oscillations. The quantum of these oscillations is referred to as surface plasmon. A large number of negatively charged free electrons exists inside a conductor (free electron charge density is 10^{23} cm^{-3}) with an equally charged positive ion lattice. Since positive ions have an infinitely large mass compared to these free electrons, these ions can be replaced by a positive constant background. However, the total charge density inside the conductor still remains zero. If the density of free electrons is perturbed by applying an external field on the conductor, movement of free electrons may take place and they begin to get attracted by the positive ion background. This attraction acts as a driving force for free electrons and they start moving towards positive region and accumulate with a density higher than necessary to obtain charge neutrality. This results in the Coulomb repulsion among the moving free electrons which acts as a restoring force and produces motion in the opposite direction. The resultant of these two forces (i.e., attractive driving force and repulsive restoring force) set up the longitudinal oscillations among the free electrons, known as plasma oscillations. Surface plasmons cannot be excited by direct light over a metal-dielectric interface as their wave numbers are greater than the light wave number in the dielectric. Special geometries are used to excite the surface plasma waves using TM-polarized light. When TM-polarized light is incident on the glass-metal interface within the range of incidence angles, total internal reflection occurs. If the wave vector of the incident light matches the electron oscillation frequency of the metal film surface, the incident light will be coupled to the plasma surface and an electronic resonance is produced. Therefore light energy is absorbed and the intensity of reflected light reduces, so the resonant excitation of surface plasmons can be seen as the dip in reflected light intensity at a certain incident angle, which is known as the resonance angle of SPR. This resonance angle is different for various combinations of the refractive index (RI) of the metal and dielectrics and is very sensitive to the RI changes in the vicinity of a surface. Fiber optic sensors based on SPR phenomenon have been studied extensively in the field of physical, biological and chemical sensing [9–13].

2.3 Lossy Modes and Lossy Mode Resonance

Similar to the SPR phenomenon, a substrate coated with metal oxides, such as indium tin oxide (ITO) [14–16], titanium dioxide (TiO_2) [17], indium oxide (In_2O_3) [18] or polymers [15, 19] in contact with other dielectric media of higher RI, support many number of modes called lossy modes or long range guided modes leading to the phenomenon of LMR. These lossy modes are guided in the thin film and can be generated with both TE and TM polarized light. Based on detailed mode analysis, it was reported that if thin film thickness is increased, lossy modes cross the cut-off condition and start guiding in the thin film leaving the fiber core [5, 20, 21]. In the lossy mode resonance (LMR), coupling between a waveguide mode and a specific lossy mode of thin film takes place at a particular value of film thickness. This coupling requires two conditions to be satisfied, one is the condition of mode fields overlapping and the other one is the phase matching condition. In the phase matching condition, real part of propagation constant of the lossy mode should be equal to the real part of propagation constant of the waveguide mode. In order to completely understand the LMR phenomenon, one can analyze the evolution of modal effective index in the form of evanescent wave which is given as

$$n_{eff} = n_s sin\theta \tag{2}$$

where n_s is the RI of glass substrate and θ is the angle of incidence. Therefore, the effective index of evanescent wave can be modified by changing either the angle of incidence or the wavelength of incident light. At a particular angle or wavelength, the effective index of evanescent wave matches with the effective index of lossy modes and the coupling between evanescent wave and the lossy modes becomes maximum. As a consequence of maximum coupling, LMR is generated at a particular value of thin film thickness resulting in attenuation dips in the transmission spectra.

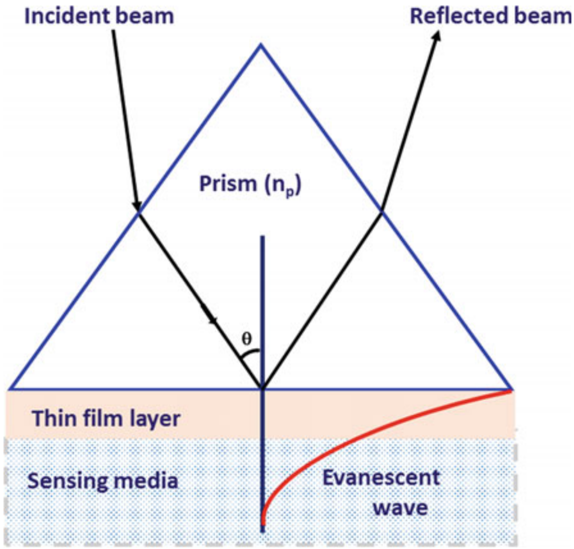

Fig. 2 Kretschmann configuration

2.4 Kretschmann-Reather ATR Method for LMR Generation

Kretschmann configuration which is shown in Fig. 2, is the most popular attenuated total reflection (ATR) method for coupling of the waveguide mode and the modes guided in the thin film coated on a prism base [22]. When a light is incident on a prism at an angle greater than the ATR angle, an evanescent wave is generated at the prism-film layer interface. The coupling between evanescent wave and thin film modes takes place under certain conditions, leading to the phenomenon of LMR. If the phase matching and mode field overlapping conditions are satisfied, the effective coupling between thin film modes and an evanescent wave takes place which results in the transfer of energy from waveguide modes to lossy modes leading to a dip in the reflected light intensity. This dip in the normalized reflected power occurs at a particular incident angle or wavelength of light due to maximum transfer of energy from the waveguide modes to lossy modes. This specific angle and wavelength are called resonance angle (θ_{res}) and resonance wavelength (λ_{res}) respectively.

2.5 LMR Sensing Principle and Performance Parameters

The principle of LMR sensing is based on either angular interrogation or wavelength interrogation. Angular interrogation utilizes various angles of incidence for the measurement of reflectance while keeping the frequency of incident light fixed. In this method, reflectance is minimum at a particular angle of incidence which is called the resonance angle (θ_{res}). This θ_{res} is generally sensitive to the surrounding medium

Fig. 3 Reflection spectra obtained with two surrounding medium refractive indices n_s and $n_s + \delta n_s$

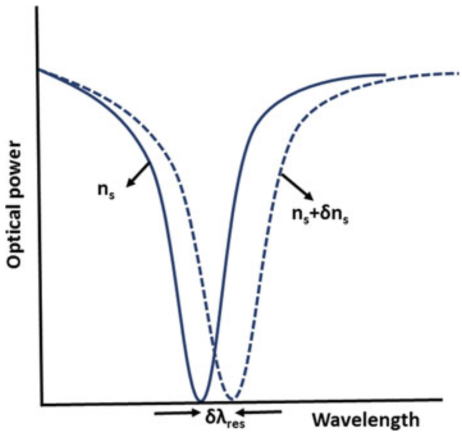

refractive index (SRI) variations. Consequently, determination of dielectric constant of surrounding medium is possible if the dielectric constant and thickness of the thin film layer are known. On the other hand, wavelength interrogation utilizes various wavelengths for the reflectance measurement while keeping the angle of incidence fixed. In this method, a broadband light source is generally used for launching the light and minimum reflectance is measured at a particular wavelength. This specific wavelength is called the lossy mode resonance wavelength (λ_{res}). The performance of an LMR based sensor is characterized by its sensitivity and detection accuracy. A perfect LMR sensor has the high sensitivity and high detection accuracy. Sensitivity of an LMR based RI sensor is given by the shift in resonance angle or the wavelength with respect to the SRI variation. It means that, large change in the resonance angle or wavelength shift leads to better sensitivity of the LMR sensor. The reflectance curves for two SRIs viz., n_s and $n_s + \delta n_s$ are shown in Fig. 3. These curves can be used to find out the λ_{res} or λ_{res} and sensitivity can be calculated from the angular or wavelength interrogation method by the following relations

$$S_\lambda = \frac{\delta \lambda_{res}}{\delta n_s} \text{..........(Wavelength interrogation)} \tag{3}$$

$$S_\theta = \frac{\delta \theta_{res}}{\delta n_s} \text{..........(Angular interrogation)} \tag{4}$$

The Second performance parameter viz., detection accuracy is defined by the ability of an LMR sensor to determine the resonance angle/wavelength accurately. Therefore, better detection accuracy provides a precise detection of the resonance angle/wavelength to determine the unknown SRI. Detection accuracy is inversely proportional to the width of LMR curve and therefore narrower LMR curve provides a better detection accuracy besides the detection limitations of the measurement device.

3 Advantages of LMR over SPR

LMR based devices have the following major advantages over the SPR based devices:

1. LMR does not require specific polarization of light and can be generated with both TE and TM polarized light while SPR can be generated only by TM polarized light.
2. Choice of materials is unlimited as most thin film materials have real part of thin film permittivity positive and higher in magnitude than both the imaginary part of the permittivity and the surrounding medium. Therefore unlike SPR, specific plasmonic materials like silver and gold are not required.
3. It is possible to generate multiple LMRs or attenuation dips in the transmittance spectra by increasing the thickness of coating material. The advantage of this feature is that sensitivity to the measurand can be tuned by just changing the thickness of the thin film layer which is not possible in the case of SPR.

4 LMR Based Fiber Optic Sensors

During the last few decades a lot of research work have been reported on SPR, but very few authors have explored the field of LMR. For the first time, Del Villar et al. [14] proposed the LMR phenomenon for fiber optic sensing applications. Thin film material and substrate are the main ingredients in designing a sensing probe. For the substrate, optical fiber is considered to be a good choice due to its small size, light weight, immunity to electromagnetic interference (EMI), capability of multiplexing, wide operating temperature range and capability of remote sensing.

Now coming to the sensor material, ITO was the first material explored by the I. Del villar group since it satisfies the condition of LMR generation as given in Table 1. ITO is a transparent conducting oxide (TCO) and thin films of ITO are chemically stable. Also, various deposition methods such as sputtering, dip coating etc. can be used for the deposition of ITO onto the optical fiber. In addition to this, it can be seen from the dispersion curve of ITO shown in Fig. 4 that it is a suitable material for the generation of both LMR and SPR in two different spectral regions [14, 23]. Fiber optic SPR sensors fabricated with ITO coating have also been utilized in mid-IR spectral region sensing. However, these are very expensive due to the high cost of IR-light sources and detectors. On the contrary, VIS-NIR light sources and detectors are of lower cost and are easily available. Additionally, LMR based humidity sensors [15] and pH sensors [19] show comparable sensitivity to the SPR sensors. In view of the above factors ITO coated LMR fiber optic sensors have been explored for various kinds of sensing applications.

Mostly, wavelength interrogation method is used in LMR fiber optic sensors because multiple reflections take place from the core of an optical fiber due to launching of all the guided modes into the fiber. All those light rays whose incident angle are greater than the critical angle undergo TIR at the fiber-cladding interface. Criti-

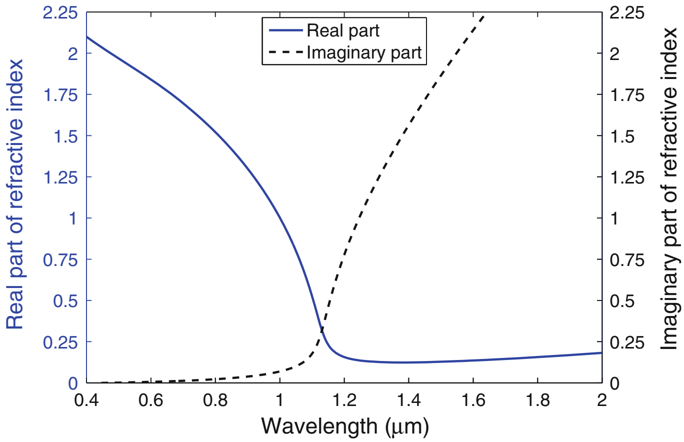

Fig. 4 Dispersion curve of ITO

cal angle is determined by the light acceptance angle or numerical aperture (NA) of the fiber and the wavelength of light. This results in the generation of an evanescent wave, which eventually couple to thin film modes under certain conditions.

Previously in some studies [6], thin film thickness was utilized to satisfy the mode cut-off condition that eventually leads to attenuation maxima of lossy modes, resulting to the LMR. However, LMR generation is also possible by launching broadband spectra into the fiber and observing the mode-cut off at a specific wavelength of spectra keeping the thin film thickness conthstant. Generally, light from a broadband source is incident at one end of the thin film coated fiber optic LMR sensing probe, and detected at the other end. Due to the LMR phenomenon attenuation dip occurs at a specific wavelength, called the resonance wavelength (λ_{res}). This λ_{res} is sensitive to the SRI variations and therefore this LMR phenomena can be utilized in RI sensors by just analyzing the λ_{res} shift in the LMR transmission spectrum. The plot of resonance wavelengths vs refractive indices of the surrounding media, provides the calibration curve for LMR fiber optic RI sensors as shown in Fig. 5.

Further, in order to completely understand the separate contribution of TE, TM and TE+TM modes in generating SPR and LMR phenomena, transmission curves have been plotted using ITO as a thin film material. As seen in Fig. 6a TE polarized light contributes only a single transmission dip appearing in the LMR's spectral region. However, TM polarized light contributes two dips appearing in two different spectral regions as shown in Fig. 6b. Among these two transmission dips, the first dip appears in LMR spectral region and the second dip in SPR region. In addition to this, the combined effect of both TE and TM modes or the unpolarized (TE+TM) light on the transmission spectra is shown in Fig. 6c. From these observations, it can be concluded that contribution of both TE and TM modes leads to the generation of LMR, whereas only TM modes contributes towards the generation of SPR as depicted in Fig. 6b. Another special feature of LMR is its ability to generate multiple LMRs with

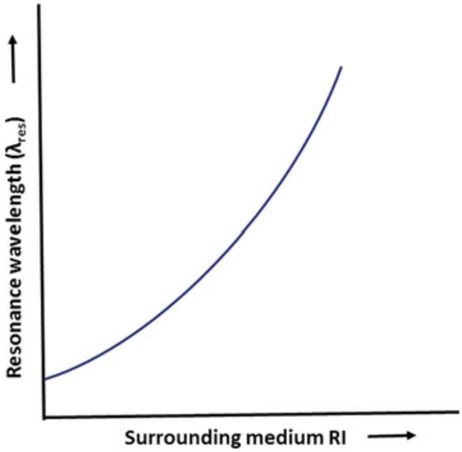

Fig. 5 Calibration curve for LMR fiber optic RI sensor

increasing thicknesses of the thin film as shown in Fig. 7a, b. This is due to the fact that on increasing the thin film thickness, multiple modes are guided in the sensing region [14] leading to the generation of multiple LMR without any modification in the fiber geometry.

5 Theoretical Model for Lossy Mode Resonance Based Fiber-Optic Sensors

This section describes a simulation model for LMR based fiber optic RI sensors with Indium tin oxide (ITO) as an LMR generating layer. Attenuated total reflection (ATR) method in combination with the well known Kretschmann configuration was used for the MATLAB simulations. Fiber parameters considered for the theoretical studies were: core diameter = 200 μm, sensing region length = 30 mm and numerical aperture (NA) = 0.22. The optical power (dP) transmitted from the fiber-end is given by [14]

$$dP \propto n_1^2 \sin\theta \cos\theta d\theta \tag{5}$$

We have considered launching of all guided rays into the fiber structure. Due to the cylindrical geometry of fiber, for the exact analysis of modes the effect of skew rays along with the meridional rays has also been taken into account. Hence, the normalized transmitted power P_t, can be written as [14]

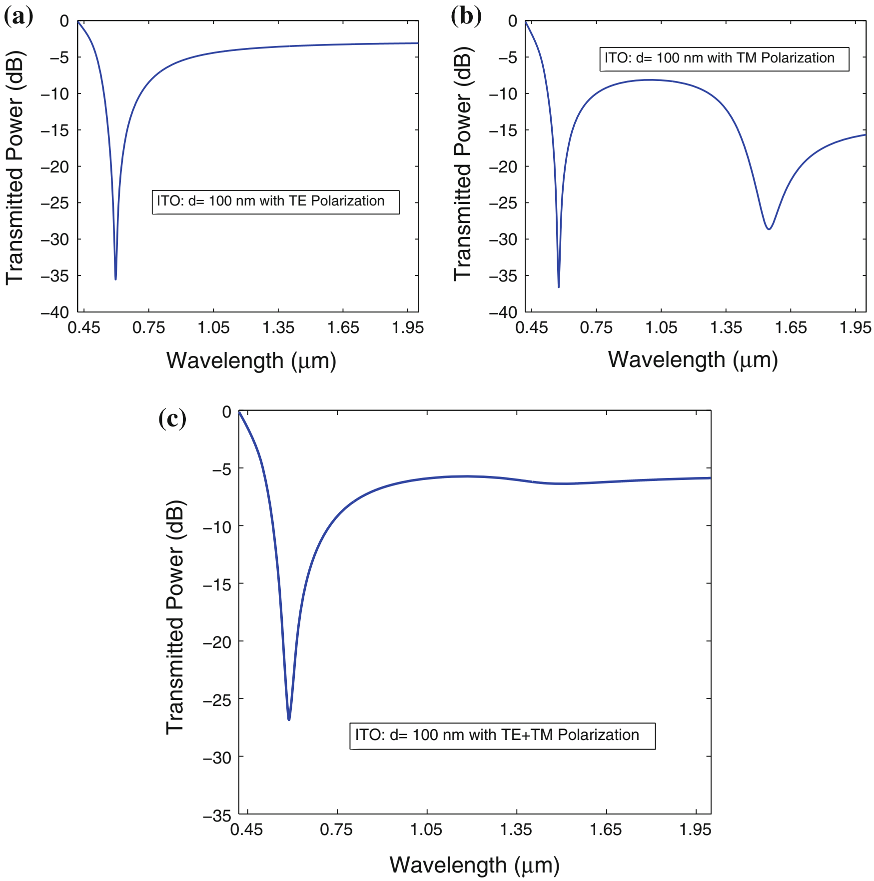

Fig. 6 (Colour Online) Theoretical transmission spectra with light of **a** TE polarization, **b** TM polarization, **c** TE+TM polarization. Other parameters are: sensing region length = 3 cm, core diameter = 200 μm, NA = 0.22, ITO layer thickness d = 100 nm and SRI = 1.33

$$P_t = \frac{\int_0^{\delta_{max}} \int_{\theta_{cr}}^{\pi/2} R^{N_{ref}(\theta,\delta)} k_0^2 n_1^2 \sin\theta \cos\theta d\theta d\delta}{\int_0^{\delta_{max}} \int_{\theta_{cr}}^{\pi/2} k_0^2 n_1^2 \sin\theta \cos\theta d\theta d\delta} \tag{6}$$

where $\theta_{cr} = \sin^{-1}\left(\frac{n_{cl}}{n_1}\right)$ is the critical angle of the fiber with n_{cl} and n_1 as the refractive indices of cladding and core respectively. $R^{N_{ref}(\theta,\delta)}(\theta, \lambda)$ is the reflected power for unpolarized light given by the expression

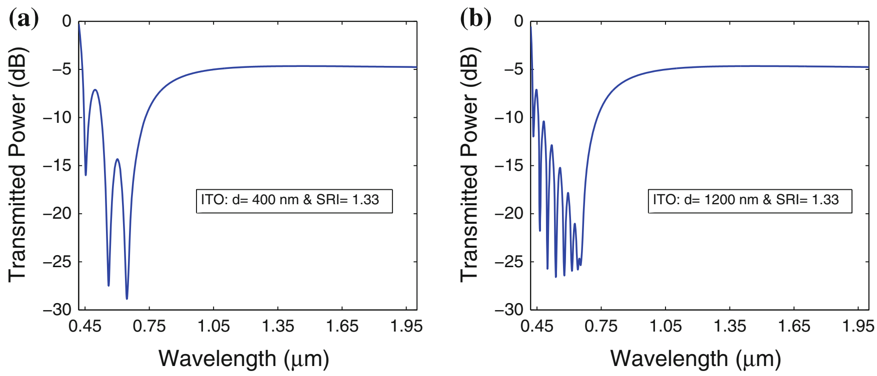

Fig. 7 (Colour Online) Theoretical multiple LMR generation by unpolarized light with ITO layer thickness of **a** d = 400 nm, **b** d = 1200 nm. Other parameters are: sensing region length = 3 cm, core diameter = 200 µm, NA = 0.22 and SRI = 1.33

$$R^{N(\theta,\delta)}(\theta,\lambda) = \frac{R_{TE}^{N(\theta,\delta)}(\theta,\lambda) + R_{TM}^{N(\theta,\delta)}(\theta,\lambda)}{2} \tag{7}$$

and $N_{ref}(\theta,\delta)$ is the number of reflections at the core- thin film interface expressed by the equation given below

$$N_{ref}(\theta,\delta) = \frac{L}{D\tan\theta\cos\delta} \tag{8}$$

Here, D is the core diameter of fiber, L is the length of sensing region, θ is the angle of incident ray with respect to the normal to core-thin film interface and δ is the skewness angle. In order to calculate the reflection intensity coefficient R(θ, λ) for unpolarized light beam, N-layer (transfer matrix) method is used [24].

5.1 *Transfer Matrix Method for a Multilayer System*

This method assumes that all thin film layers are uniform, isotropic, non-magnetic and stacked along the z-axis as shown in Fig. 8. These layers are characterized by the dielectric constant ϵ_n, permeability μ_n and thickness d_n. The tangential fields at the boundaries $Z = Z_1 = 0$ and $Z = Z_{N-1}$ are related by the relation [24].

$$\begin{bmatrix} E_1 \\ H_1 \end{bmatrix} = M \begin{bmatrix} E_{N-1} \\ H_{N-1} \end{bmatrix} \tag{9}$$

where E_1, H_1 and E_{N-1}, H_{N-1} are the tangential components of electric and magnetic fields at the first layer's boundary and the Nth layer's boundary respectively. Here,

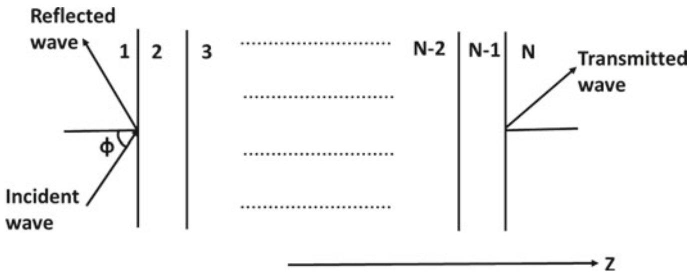

Fig. 8 N-Layers method for the calculation of reflected light intensity

M is the characteristic matrix for the multilayer structure and is given by

$$M = \prod_{n=2}^{N-1} M_n \tag{10}$$

where

$$M_n = \begin{bmatrix} \cos\beta_n & -\frac{i}{q_n}\sin\beta_n \\ -iq_n \sin\beta_n & \cos\beta_n \end{bmatrix} \tag{11}$$

and

$$q_n = \frac{\sqrt{\epsilon_n - n_1^2 \sin\phi^2}}{\epsilon_n} \text{..........(TM modes)} \tag{12}$$

$$q_n = \sqrt{\epsilon_n - n_1^2 \sin\phi^2} \text{..........(TE modes)} \tag{13}$$

$$\beta_n = \frac{2\pi d_n}{\lambda}\sqrt{\epsilon_n - n_1^2 \sin\phi^2} \tag{14}$$

The reflection amplitude for unpolarized incident light is calculated by

$$r = \frac{(M_{11} + M_{12}q_N)q1 - (M_{21} + M_{22}q_N)}{(M_{11} + M_{12}q_N)q1 + (M_{21} + M_{22}q_N)} \tag{15}$$

Therefore, reflection intensity for unpolarized light containing TE and TM modes is given by

$$R = \frac{\mid r_{TE} \mid^2 + \mid r_{TM} \mid^2}{2} \tag{16}$$

In order to calculate the refractive indices of various layers the following dispersion models were used:

5.2 Dispersion Relation of ITO Layer

The following Drude and Lorentz oscillator dispersion model was used to describe the dispersion relation of ITO.

$$\epsilon(\omega) = \epsilon_\infty - \frac{\omega_p^2}{\omega^2 + i\frac{\omega}{\tau}} + \frac{s_0\omega_0^2}{\omega_0^2 - \omega^2 + i\gamma\omega} \tag{17}$$

where $\epsilon_\infty = 3.5$ is the high frequency dielectric constant, $\omega_p = 4.557 \times 10^{15}$ rad/s is the plasma frequency, $s_0 = 1$ is the oscillator strength, $\omega_0 = 8.27 \times 10^{15}$ rad/s is the oscillator resonance frequency, $\gamma = 1.321 \times 10^{14}$ rad/s is the damping constant and $\tau = 1.324 \times 10^{-14}$ s/rad is the electronic scattering time.

5.3 Dispersion Relation of Silica

In our theoretical studies we assume that the core of the fiber is made of fused silica. The expression for the wavelength dependent refractive index of fused silica is given by the Sellmeier relation [25] as

$$n_1(\lambda) = \sqrt{1 + \frac{a_1\lambda^2}{\lambda^2 - b_1^2} + \frac{a_2\lambda^2}{\lambda^2 - b_2^2} + \frac{a_3\lambda^2}{\lambda^2 - b_3^2}} \tag{18}$$

where λ denotes the wavelength (in μm) and the Sellmeier coefficients are $a_1 = 0.6961663$, $a_2 = 0.4079426$, $a_3 = 0.8774794$, $b_1 = 0.0684043$, $b_2 = 0.1162414$ and $b_3 = 9.896161$.

The different SRIs used for the analysis were 1.33, 1.35, 1.37, 1.39, 1.41, 1.43. Wavelength interrogation method was used to obtain the LMR transmission spectra for different SRIs as shown in Fig. 9a. In order to calculate the sensitivity, resonance wavelengths can be found out from these transmission spectra. Additionally, the effect of ITO thickness on the sensitivity of LMR fiber optic RI sensor is shown in Fig. 9b. As observed in Fig. 9b spacing between LMR curves gets reduced with increasing film thickness which results in decreased sensitivity.

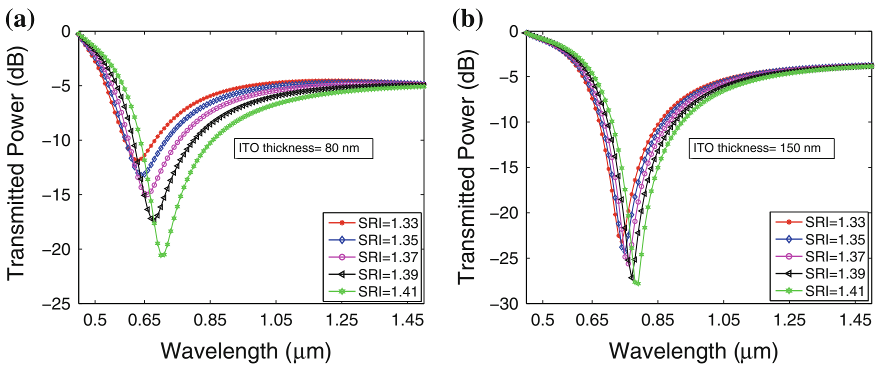

Fig. 9 (Colour Online) LMR transmission spectra obtained with different surrounding medium refractive indices (SRIs) for ITO layer thickness of **a** d = 80 nm, **b** d = 150 nm. Other parameters are: sensing region length = 3 cm, core diameter = 200 μm, NA = 0.22

6 Recent Advancenents in LMR Bsed Fiber Optic Sensors

Till 2010 LMR remained an unexplored phenomenon for fiber optic sensing applications before it was proposed by Del Villar et al. [14] for RI sensing. The sensitivity of this first LMR based RI sensor was evaluated with ITO film thickness of 115 and 220 nm using water-glycerin solutions of different RIs, whose sensitivities were found to be 1617.4 nm/RIU and 2952.6 nm/RIU respectively. A typical experimental-setup which can be used for LMR based fiber optic RI sensing is shown in Fig. 10. Here, an optical fiber is de-cladded from the middle and a thin film overlay is deposited onto the uncladded region. This fiber structure is surrounded by the medium whose RI is under investigation.

Around the same time, optical fiber refractometer based on the same ITO coating was fabricated by Zamarreno et al. [26] in which they found the sensitivity of refractometer to be independent of the sensing region length. They reported an average sensitivity of 3125 nm/RIU which was comparable to the SPR sensors. LMR phenomenon was also utilized for relative humidity sensing [15] and a tunable humidity sensor was fabricated by depositing ITO and poly allylamine hydrochloride (PAH) and poly acrylic acid (PAA) film which is sensitive to relative humidity. The sensitivities of tuned and non-tuned RH sensors were compared. Around 5 fold increase in the sensitivity was reported for the tuned RH sensor.

Due to the limitation of ITO material in generating LMR within the specific spectral range, another metal oxide TiO_2 was explored. It was discovered that TiO_2 is free from the limitations of LMR generation in specific wavelength spectrum as can be seen from the dispersion curve of TiO_2 [17]. Therefore, unlike ITO, the complete wavelength range of 500–1500 nm is available for LMR generation in TiO_2 because the real part of dielectric constant always remains positive and higher than its imaginary part for the entire wavelength spectrum. Keeping this fact in view, the

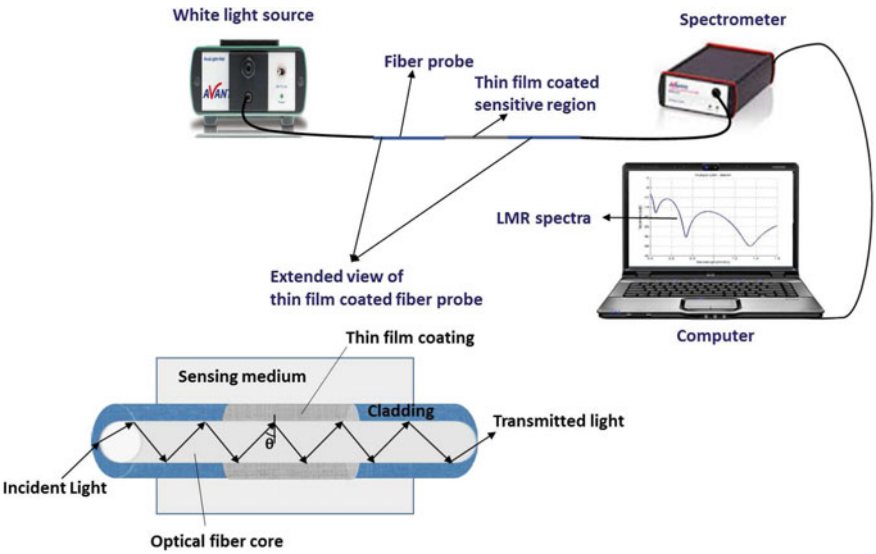

Fig. 10 Experimental setup used for LMR based fiber optic sensing

optical fiber refractometers were fabricated by depositing TiO_2/PSS (poly sodium 4-styrenesulfonate) thin films by using layer-by-layer (LbL) method. All studies on these LMR based refractometers show that thin film thickness plays an important role in determining the sensitivity. Better sensitivity can be achieved if thin film thickness is kept less. Consequently, the major advantage of LMR based fiber optic refractometers is that sensitivity, position and number of transmission dips can be fine tuned by just changing the film thickness. Also, another composite oxide material indium oxide (In_2O_3) was studied for LMR generation and it was reported that with In_2O_3 dual peak LMR can be generated which is useful for performing very precise measurements with better accuracy and two fold sensitivity enhancement [18]. Besides RI and RH measurements, LMR phenomenon had also shown its potential in pH sensing [19]. For the fabrication of LMR based pH sensor, PAH/PAA coatings were chosen because LMR can be generated with these polymers. Also, PAH/PAA thin films are suitable for pH measurement because thickness of these films increase or decrease with the pH variation of the solution which causes the SRI change. A fairly good sensitivity of 0.027 pH units/nm with an accuracy of 0.001 pH units was achieved with this pH sensor for a pH range of 3–6. Though, many materials including metal oxides and polymers were explored for various physical and chemical sensing utilizing LMR phenomena, some other design parameters which affect the sensitivity and resolution of these LMR sensors also need to be addressed. Therefore, to achieve the better performance of LMR sensor some design studies were presented [27]. For the optimization of LMR sensing design parameters, TiO_2/PSS and PAH/PAA were chosen because both these materials are suitable for LMR generation. In these studies it was concluded that only the real part of thin film RI is responsible for the wavelength shift which eventually provides the sensitivity of the LMR device. However, the imaginary part of thin film RI accounts for the losses occurring in the structure and thus the depth of resonance curve. Hence, there is no role for the imaginary part of the thin film RI in determining the sensitivity of an LMR device. As we know thin film properties drastically vary with the deposition techniques [28–30], ITO coated LMR based optical fiber refractometer was also studied where ITO was deposited by sputtering technique unlike LbL and dip coating techniques reported in literature [14, 15, 17]. After the successful development of pH, RH and RI sensors, fiber optic immunoglobulin G (IgG) biosensor was reported utilizing LMR phenomena [31]. This biosensor was fabricated by depositing PAH/PSS thin films because these films provide a suitable medium for IgG-anti-IgG immunoreactions and also capable of generating LMR. With this IgG biosensor, 50 μg/ml concentration of Immunoglobulins were detected in a response time of 12 min. In an another work, a new LMR based fiber optic RH sensor was reported in which multiple LMR phenomena was utilized as a notch band filter [32]. Further, in order to show the effect of fiber geometry, the use of side-polished, D-shaped single mode fiber (SMF) coated with TiO_2/PSS was reported for fiber based LMR devices [33]. Their experimental results demonstrate the importance of D-shape SMF in determining the individual contribution of TE and TM polarizations in LMR generation.

A different kind of LMR based chemical vapor sensor for the detection of volatile organic compounds (VOCs) was developed by depositing an organometallic compound $[Au_2Ag_2(C_6F_5)_4(C_6H_5C\equiv CC_6H_5)_2]_n$ which is sensitive to organic vapors [34]. The performance of this sensor was evaluated with different concentrations of ethanol, methanol and isopropanol vapors taking the effect of humidity and temperature into account. Furthermore, for monitoring human breath an LMR based sensor was designed with silver nanoparticle loaded films onto the fiber [35]. The dynamic range of 27.3 nm and sensitivity of 0.455 nm/RH% was achieved for this human breath sensing device.

All the LMR sensors discussed so far utilized only a single LMR generating thin film layer. In order to enhance the sensitivity of an LMR device, fiber optic RI sensors with bilayer combination of ITO/TiO_2 was theoretically investigated [36] using transfer matrix method described in Sect. 5.1. This work reports the capability of combined ITO and TiO_2 thin films in enhancing the RI sensitivity when combined in a particular ratio. A comparison of sensitivity was carried out utilizing ITO/TiO_2 bilayer and single absorbing layer in LMR based RI sensors. It was concluded from these theoretical studies that with ITO/TiO_2 bilayer combination, a much better sensitivity can be achieved as compared to single absorbing layer. An another LMR based biosensor was reported for thrombin and C-reactive protein detection [37, 38]. Again in another work, two different bilayer combinations viz. AZO/TiO_2 and AZO/Cu_2O were theoretically investigated for the enhancement of RI sensitivity [39] and AZO/TiO_2 was reported to be a much better combination for increasing the RI sensitivity up to five fold.

Another important LMR based biosensor was reported for the diagnosis of celiac disease [40]. This work was carried out first utilizing different geometries of the fibers and then choosing the appropriate geometry for fabrication of the biosensor. Among all the geometries, best detection accuracy was achieved with tapered single-mode optical fibers (T-SMFs). These T-SMFs were used to fabricate the sensing device to detect anti-gliadin antibodies (AGAs) for the diagnosis of celiac disease. The devices fabricated in this work have the potential for other biological and chemical applications. LMR phenomena was also theoretically exposed for temperature sensing [41]. In this work, TiO_2 coated LMR based fiber optic temperature sensor was reported and the sensitivity was evaluated by considering air and water as the surrounding media. The role of different TiO_2 thicknesses in determining the sensitivity was discussed. As compared to fiber Bragg grating (FBG) and localized surface plasmon resonance (LSPR) based fiber optic temperature sensors [42, 43], the proposed sensor promises higher temperature sensitivity with 100 nm thickness of TiO_2. The major benefit of LMR based temperature sensor is that, it does not require an extra metal layer unlike FBG and LSPR temperature sensors and its sensitivity can be tuned by just changing the TiO_2 thickness. Recently, improvement in the reduction of spectral width by utilizing D-shaped optical fibers for fabrication of LMR based refractometers was reported [44]. This work presented a highly sensitive ITO coated D-shaped optical fiber refractometer with very narrow spectral width and high attenuation of 6.9 nm and 36 dB. In a recent review article a detailed analysis of LMR phenomena along with its major fields of applications was reported [45].

7 Conclusion

This chapter presents details of the LMR phenomena and considered various designs and performance parameters for LMR based fiber-optic sensors. The basic principle of LMR based fiber-optic sensors was explained and various benefits such as sensitivity and detection accuracy enhancement by using double thin film layers, tapered and D-shape geometry for LMR based fiber-optic sensors were addressed. The popularity of LMR sensors is primarily based on two reasons: first, these are free from the requirement of specific polarization of light, and secondly due to the capability of tuning its sensitivity by just adjusting thickness of the thin film. Also, another exclusive property of LMR devices is multiple LMR generation with increasing thickness which can be utilized in wavelength filtering applications. LMR technology has motivated research on the geometry of fiber optic probe for further enhancing the sensitivity and detection accuracy for various sensing applications. LMR cannot be considered just a cost effective solution in the field of sensing as all the LMR generating materials show high sensitivity in the NIR spectral range. This calls for future research of suitable materials with enhanced sensitivity of LMR sensors in the visible spectral region. LMR phenomena can also be explored with other nanoparticle based sensing techniques like LSPR. In view of all these LMR based fiber optic sensing technology would be a very promising research field. The present chapter is a small attempt to provide an insight into the recent advancements in this emerging field. Fiber optic sensor technology promises bright future prospects with significant advancements in the coming years. LMR based fiber-optic sensors are expected to be a major contributor to the sensing research community with comparably high sensitivity along with its various advantages over the other fiber optic sensors.

References

1. A. Kersey, A. Dandridge, Applications of fiber-optic sensors. IEEE Trans. Compon. Hybrids Manuf. Technol. **13**(1), 137–143 (1990)
2. B. Culshaw, A. Kersey, Fiber-optic sensing: a historical perspective. J. Lightwave Technol. **26**(9), 1064–1078 (2008)
3. R. Bogue, Fibre optic sensors: a review of today's applications. Sens. Rev. **31**(4), 304–309 (2011)
4. B. Lee, S. Roh, J. Park, Current status of micro- and nano-structured optical fiber sensors. Opt. Fiber Technol. **15**(3), 209–221 (2009)
5. T. Batchman, G. McWright, Mode coupling between dielectric and semiconductor planar waveguides. IEEE Trans. Microwave Theory Tech. **30**(4), 628–634 (1982)
6. M. Marciniak, J. Grzegorzewski, M. Szustakowski, Analysis of lossy mode cut-off conditions in planar waveguides with semiconductor guiding layer. Optoelectr. IEE Proc. J. **140**(4), 247–252 (1993)
7. T. Takano, J. Hamasaki, Propagating modes of a metal-clad-dielectric-slab waveguide for integrated optics. IEEE J. Quantum Electr. **8**(2), 206–212 (1972)
8. F. Yang, J.R. Sambles, Determination of the optical permittivity and thickness of absorbing films using long range modes. J. Modern Opt. **44**(6), 1155–1163 (1997)
9. J. Homola, S.S. Yee, G. Gauglitz, Surface plasmon resonance sensors: review. Sens. Actuators B: Chem. **54**, 3–15 (1999)
10. A.K. Sharma, R. Jha, B.D. Gupta, Fiber-optic sensors based on surface plasmon resonance: a comprehensive review. Sens. J. IEEE **7**(8), 1118–1129 (2007)
11. A. Leung, P.M. Shankar, R. Mutharasan, A review of fiber-optic biosensors. Sens. Actuators B: Chem. **125**(2), 688–703 (2007)
12. X.D. Wang, O.S. Wolfbeis, Fiber-optic chemical sensors and biosensors (2008–2012). Anal. Chem. **85**(2), 487–508 (2013)
13. I. Abdulhalim, M. Zourob, A. Lakhtakia, Surface plasmon resonance for biosensing: a mini-review. Electromagnetics **28**(3), 214–242 (2008)
14. I.D. Villar, C.R. Zamarreno, M. Hernaez, F.J. Arregui, I.R. Matias, Lossy mode resonance generation with indium-tin-oxide-coated optical fibers for sensing applications. J. Lightwave Technol. **28**(1), 111–117 (2010)
15. C.R. Zamarreno, M. Hernaez, I.D. Villar, I.R. Matias, F.J. Arregui, Tunable humidity sensor based on ITO-coated optical fiber. Sens. Actuators B: Chem. **146**(1), 414–417 (2010)
16. D. Kaur, V. Sharma, A. Kapoor, High sensitivity lossy mode resonance sensors. Sens. Actuators B: Chem. **198**, 366–376 (2014)
17. M. Hernaez, I.D. Villar, C.R. Zamarreno, F.J. Arregui, I.R. Matias, Optical fiber refractometers based on lossy mode resonances supported by TiO_2 coatings. Appl. Opt. **49**, 3980–3985 (2010)
18. I.D. Villar, C.R. Zamarreno, P. Sanchez, M. Hernaez, C.F. Valdivielso, F.J. Arregui, I.R. Matias, Generation of lossy mode resonances by deposition of high-refractive-index coatings on uncladded multimode optical fibers. J. Opt. **12**(9), 095503 (2010)
19. C.R. Zamarreno, M. Hernaez, I.D. Villar, I.R. Matias, F.J. Arregui, Optical fiber pH sensor based on lossy-mode resonances by means of thin polymeric coatings. Sens. Actuators B: Chem. **155**(1), 290–297 (2011)
20. R.F. Carson, T.E. Batchman, Multimode phenomena in semiconductor-clad dielectric optical waveguide structures. Appl. Opt. **29**(18), 2769–2780 (1990)

21. I.D. Villar, I.R. Matias, F.J. Arregui, M. Achaerandio, Nanodeposition of materials with complex refractive index in long-period fiber gratings. J. Lightwave Technol. **23**(12), 4192–4199 (2005)
22. E. Kretschmann, H. Reather, Radiative decay of non-radiative surface plasmons excited by light. Zeitschrift fur Naturforschung **23**, 21352136 (1968)
23. I.D. Villar, C.R. Zamarreno, M. Hernaez, P. Sanchez, F.J. Arregui, I.R. Matias, Generation of surface plasmon resonance and lossy mode resonance by thermal treatment of ITO thin-films. Opt. Laser Technol. **69**, 1–7 (2015)
24. J. Chilwell, I. Hodgkinson, Thin-films field-transfer matrix theory of planar multilayer waveguides and reflection from prism-loaded waveguides. J. Opt. Soc. Am. A **1**(7), 742–753 (1984)
25. G.P. Agarwal, *Nonlinear Fiber Optics*, 3rd edn. (Academic, New York, 2001)
26. C.R. Zamarreno, M. Hernaez, I.D. Villar, I.R. Matias, F.J. Arregui, ITO coated optical fiber refractometers based on resonances in the infrared region. Sens. J. IEEE **10**(2), 365–366 (2010)
27. I.D. Villar, M. Hernaez, C.R. Zamarreno, P. Sanchez, C. Fernandez-Valdivielso, F.J. Arregui, I.R. Matias, Design rules for lossy mode resonance based sensors. Appl. Opt. **51**(19), 4298–4307 (2012)
28. S.H. Brewer, S. Franzen, Optical properties of indium tin oxide and fluorine-doped tin oxide surfaces, correlation of reflectivity, skin depth, and plasmon frequency with conductivity. J. Alloys Compd. **338**, 73–79 (2002)
29. I. Hamberg, A. Hjortsberg, C. Granqvist, High quality transparent heat reflectors of reactively evaporated indium tin oxide. Appl. Phys. Lett. **40**(5), 362–364 (1982)
30. S. Laux, N. Kaiser, A. Zoller, R. Gotzelmann, H. Lauth, H. Bernitzki, Room-temperature deposition of indium tin oxide thin films with plasma ion-assisted evaporation. Thin Solid Films **335**, 1–5 (1998)
31. A. Socorro, J. Corres, I.D. Villar, F.J. Arregui, I.R. Matias, Fiber-optic biosensor based on lossy mode resonances. Sens. Actuators B: Chem. **174**, 263–269 (2012)
32. P. Sanchez, C.R. Zamarreno, M. Hernaez, I.D. Villar, I.R. Matias, F.J. Arregui, Considerations for lossy-mode resonance-based optical fiber sensor. Sens. J. IEEE **13**(4), 1167–1171 (2013)
33. C.R. Zamarreno, P. Zubiate, M. Sagues, I.R. Matias, F.J. Arregui, Experimental demonstration of lossy mode resonance generation for transverse-magnetic and transverse-electric polarizations. Opt. Lett. **38**(14), 2481–2483 (2013)
34. C. Elosua, I. Vidondo, F.J. Arregui, C. Bariain, A. Luquin, M. Laguna, I.R. Matias, Lossy mode resonance optical fiber sensor to detect organic vapors. Sens. Actuators B: Chem. **187**, 65–71 (2013)
35. P.J. Rivero, A. Urrutia, J. Goicoechea, I.R. Matias, F.J. Arregui, A lossy mode resonance optical sensor using silver nanoparticles-loaded films for monitoring human breathing. Sens. Actuators B: Chem. **187**, 40–44 (2013)
36. N. Paliwal, J. John, Theoretical modeling of lossy mode resonance based refractive index sensors with ITO/TiO_2 bilayers. Appl. Opt. **53**, 3241–3246 (2014)
37. C.R. Zamarreno, I. Ardaiz, L. Ruete, F. Munoz, I.R. Matias, F.J. Arregui, C-reactive protein aptasensor for early sepsis diagnosis by means of an optical fiber device. Sens. IEEE **2013**, 1–4 (2013)
38. L. Razquin, C.R. Zamarreno, F. Munoz, I.R. Matias, F.J. Arregui, Thrombin detection by means of an aptamer based sensitive coating fabricated onto LMR-based optical fiber refractometer. Sens. IEEE **2012**, 1–4 (2012)
39. N. Paliwal, J. John, Sensitivity enhancement of aluminium doped zinc oxide (AZO) coated lossy mode resonance (LMR) fiber optic sensors using additional layer of oxides. Frontiers in Optics. Optical Society of America, p. JTu3A.40 (2014)
40. A. Socorro, I.D. Villar, J. Corres, F.J. Arregui, I.R. Matias, Spectral width reduction in lossy mode resonance-based sensors by means of tapered optical fibre structures. Sens. Actuators B: Chem. **200**, 53–60 (2014)
41. N. Paliwal, J. John, Theoretical modelling of lossy mode resonance (LMR) based fiber optic temperature sensor utilizing TiO_2 sensing layer. in *12th International Conference on Fiber Optics and Photonics* (Optical Society of America, 2014), p. M4A.22

42. S.K. Srivastava, B.D. Gupta, Simulation of a localized surface-plasmon-resonance-based fiber optic temperature sensor. J. Opt. Soc. Am. A **27**(7), 1743–1749 (2010)
43. N. Liu, Y. Li, Y. Wang, H. Wang, W. Liang, P. Lu, Bending insensitive sensors for strain and temperature measurements with bragg gratings in bragg fibers. Opt. Exp. **19**(15), 13 880–13 891 (2011)
44. P. Zubiate, C.R. Zamarreno, I.D. Villar, I.R. Matias, F.J. Arregui, High sensitive refractometers based on lossy mode resonances (LMRs) supported by ITO coated D-shaped optical fibers. Opt. Exp. **23**(6), 8045–8050 (2015)
45. N. Paliwal, J. John, Lossy mode resonance (LMR) based fiber optic sensors: a review. Sens. J. IEEE **15**(10), 5361–5371 (2015)

http://www.springer.com/978-3-319-42624-2

Fiber Optic Sensors
Current Status and Future Possibilities
Matias, I.R.; Ikezawa, S.; Corres, J. (Eds.)
2017, VIII, 381 p. 221 illus., Hardcover
ISBN: 978-3-319-42624-2